INVESTIGATION INTO OPTIMISING INTENSE MUON SOURCES FOR HIGH ENERGY PHYSICS

3rd Year Project Report

Camilla Compton 00835842

Project Supervisor: Ajit Kurup

19th January 2016

Contents

Abstract

Through the simulation of firing a high energy Proton beam into a target, muon production has been studied. With the aim of improving the muon beam intensity, possible optimisations to the beam and target design of the proposed NF have been investigated. The optimum effective mercury target length was found to be 500mm. Increasing proton beam kinetic energy was found to increase both the total muon yield and the escaping particle's momentum. An increase momentum reduces the percentage captured; thus it would be unnecessary to increase the proton beam to energies above 13GeV, dependent on validity of the simulation, and the construction of the Neutrino Factory. A target constructed by layering different materials was investigated, however, no significant increases to particle yield were found. These effects would have to be reviewed in greater detail in order conclude their merit.

1 Introduction and Aims

Muons are a necessary tool in many areas of current Physics research. Generally, muons sources run at a low energy and yield in order to study material and substance samples: muons coming to rest and decaying inside the sample in question can non-intrusively give information on the characteristics of materials, for example nuclear charge distributions [1][2]. Conversely, this study will look at high energy and yield sources for the analysis of neutrinos created from muon decays. Specifically, the proposed Neutrino Factory (NF), which utilizes muon-neutrino decays and is hoped to give an alternative source from which to carry out neutrino investigations. A source of this type is necessary as there are still many theories about neutrinos which are not fully understood.

Both these methods of high or low energy muon production are technically the same. The process of muon creation is via a spallation reaction, where a proton beam, upon impact with a material target, breaks it up into other particles which are ejected. The difference is in the initial energy of the proton beam which determines whether the muons are created as a 'surface' beam as in material studies or a 'decay beam' as used to create neutrinos [2].

There are many existing muon sources. Most notably are SNS in Tennessee with the world's most intense source of pulsed muons [4], ISIS in Oxfordshire with a proton beam energy of 800MeV [5], J-Parc in Japan with a 3GeV proton beam who currently produce neutrinos from muons, and PSI in Switzerland which is a 590MeV cyclotron that delivers a 1.3MW proton beam: the most powerful proton accelerator and continuous muon source in the world [6]. The NF would be more efficient as muons of both signs can be collected and so running times can be reduced. Other facilities would have to switch running modes, making the NF a desired source.

In order for experiments at the NF to be of the required sensitivity, the number of neutrino decays needs to be 10^{21} per year [3]. This high number, in turn, determines the necessary power of the initial proton beam. This is more achievable by increasing the captured muon yield for any given number of initial protons. Due to the scattering mechanisms inside the target all the particles are emitted travelling in a range of directions. Muons are captured via a magnetic field produced by solenoids surrounding the target [3]. If the muon is not travelling predominantly in its original direction, the magnetic field will not be strong enough to capture it. These particle loses must be taken into account when calculating the yield of the system. The aim is to find the optimum beam energy and target design to give the highest captured muon yield in order to consequently maximize the neutrino beam sensitivity and thus quality of neutrino investigations. The NF has been designed but funds for construction are currently unavailable. If it can be demonstrated that the factory would have an increased sensitivity, then this would make the project a more viable option for future investment.

This study will look at the methods behind muon production and the current design for the proposed Neutrino factory. The method of modelling and simulation will be described before investigation of the main parameters of the target system: geometry, composition and beam energy. Following investigations, further studies will be completed in order to optimise the target system.

2 Theory

2.1 High Energy Interactions in Matter

Incoming particles undergo different types of interactions within matter. They are hence scattered off atoms within the material, primarily via inelastic and elastic scattering.

2.1.1 Inelastic Scattering

During inelastic scattering, a reaction takes place meaning the incident and outgoing particles are different. An example is pion production, where an incident high energy proton from the beam collides with a nucleon from the target, creating a pion by

$$p + p \rightarrow p + n + \pi^+ \tag{1}$$

or

$$p + n \rightarrow n + n + \pi^+. \tag{2}$$

This reaction requires the incoming proton to have a minimum energy of $290MeV$. At low energies, to conserve the +1 charge of the incoming proton, only π^+ will be produced. There are many other production processes that can produce both single and multiple pions: at higher energies, the proton, on interacting with atomic nuclei in the target, can produce a π^+ and additionally one or many $\pi^+\pi^-$ pairs. This is allowed by charge conservation as the pion pairs are always created together. For this reason it is expected that, as the energy of protons incident on a target increases, the yield of pions subsequently increases because more pairs of pions can be produced.

2.1.2 Elastic Scattering

During elastic scattering the total kinetic energy of the system in the centre of mass frame is conserved meaning no particles are destroyed or made in the interaction. This is the method by which the protons in the initial beam and the subsequently produced pions most predominantly lose their energy. This happens by ionisation, where an electron is liberated from an atom in the target and a 1+ ion is created:

$$X + p \rightarrow X^+ + p + e^-. \tag{3}$$

Often energy loss of this type merely excites the atom rather than ionising it [7]:

$$X + p \rightarrow X^* + p \tag{4}$$

Either process has the same effect on the incoming particle: it loses energy [8].

Once pions have been produced they have a mean lifetime of 2.6×10^{-8}s [9] before they decay into a muon of the same charge. The primary decay modes primary decay modes occur with a probability of 0.99877 [9]. These are given by

$$\pi^+ \rightarrow \mu^+ + \nu_\mu \tag{5}$$

and

$$\pi^- \rightarrow \mu^- + \bar{\nu}_\mu. \tag{6}$$

For a pion travelling at the speed of light in a vacuum, the decay would occur at an average distance of 7.8m. The pion decays are three body decays meaning the energy and momentum of the muons produced are fixed in the centre of mass frame [8]. The muons produced in these decays have a mean lifetime of 2.2×10^{-6}s: a relatively long amount of time in subatomic particle Physics [10].

2.2 Neutrino Factory Design

The basic design for the proposed NF is a high power 4MW pulsed proton beam with a RMS radius of 1.2mm, incident on a liquid mercury jet target. The collisions inside the target will produce high energy pions which are captured by a strong 20T magnetic field. Other particles will be removed via bending magnets and the pions will decay into muons before being separated into bunches and accelerated to 10GeV. At this point the muons can be injected into a decay ring where they are stored until they decay into neutrinos; the majority of these decays would happen in straight sections of the decay ring, creating a neutrino beam that will leave the ring and be observed by detectors around 2000km away. It is anticipated that through these observations very high sensitivity neutrino studies will be possible. The aim of the project is to obtain 10^{21} neutrino decays per year.

It is expected that in order to generate a sufficient pion yield the proton beam will need to consist of $3\times$ 4mW bunches of protons, equivalent to 3.125×10^{15} protons per second, with a 50Hz repetition rate, and the kinetic energy of the beam will be between 5 and 15GeV. This is a very large range of kinetic energies and is due to the large effect that energy has on the interactions which occur inside the target, and thus on the behaviour, type and yield of the created particles. This is described in Section 2.1 and is the reason the exact optimum kinetic energy is as yet unknown. The NF design report [3] does not need to state the required kinetic energy because the current, where current is the number of protons in each bunch, produced by the photon driver can be scaled dependent on the value of optimum kinetic energy found. This would importantly keep the power and thus the number of necessary neutrinos at the required value.

The design states that a liquid mercury should be used as the target material. This is due to the high atomic number of mercury giving a high pion production as outlined in Section 4.3. Additionally, a solid target would be damaged by the high power of the protons. The MERIT collaboration has proved the feasibility of such a design [11]. The requirement for a liquid target restricts the materials that the target can be constructed from. A liquid lead–bismuth target was successfully produced in the MEGAPIE test experiment at PSI. This may be a viable NF alternative as it is less toxic than mercury and its higher melting point (400^{o}C design temperature) means the liquid would solidify at room temperature, reducing the risks of any hazardous leaks [12]. The jet will have an RMS radius of 5mm and an effective length to the proton beam of around 30cm.

The target system will need to include significant shielding from radiation due to the high power of the proton beam causing high levels of activation in the materials surrounding the target. Such shielding would increase the lifespan of the solenoids. The shielding would also act as a safety feature to absorb the high quantity of harmful neutrons and gamma rays that are created in the proton-target interaction.

A strong 20T magnetic field surrounds the target to capture both the positively and negatively charged pions and muons. To achieve this high field strength an extremely strong hybrid magnet would need to be used. The stored magnetic energy would be 3GJ. This very high value results in large safety concerns as this stored energy would need to be dissipated without danger if the magnet was to quench: where superconducting properties terminate. The field in the NF design tapers down from 20T to 1.5T over a distance of 15m while the beam pipe radius increases from 75mm to 300mm. After this point, the lower momentum pions and muons are deflected by bending magnets to remove the other particles. The magnetic field then remains constant for 40.8m, giving all the remaining pions time to decay into muons.

Once the beam consists purely of muons, they are manipulated into bunches with low divergence before being accelerated to 10GeV by a series of linear accelerators which work by using oscillating electric fields. At this energy the muons can be injected into the decay ring until they form the neutrinos desired by the project.

3 Method

3.1 Simulation Software

The study uses simulations of the proposed NF source created with the beam tracking simulation g4beamline. This is a user interface for the GEANT4 code which uses Monte Carlo methods. The code is active: experimental data is used to improve its accuracy to observed interactions. It is currently used to simulate experiments at CERN, Fermilab, and for many other applications in and outside of High Energy Physics [13] [14].

The GEANT4 code models the trajectory of the incident particles individually. Statistical models are used to simulate the interactions occurring; together with the trajectories and further interactions of any subsequently created particles.

In the simulation the initial position, direction, energy and particle type of the incident beam can be individually specified. Additionally, a target of a chosen material and detectors can be arranged as required. Virtual detectors are positioned tightly encasing the target. These measure particle type, position and momentum in three-dimensions for every particle passing through them without effect to the particle; thus the state of particles at the instant they leave the target is known.

The GEANT4 code can use several different physics lists to model the interactions that take place. They each use slightly different statistical models for different energy ranges. This is necessary because a single fully functioning model of interactions for all particles and energies has yet to be found. The physics list QGSP_BERT is used in this study as it has been found to best agree with experimental data. Within this list, the Geant4 Bertini cascade model is used for primary protons, neutrons, pions and kaons below around 10GeV. An alternate model, the quark gluon string model, is used above 10GeV [14]. The discrepancy caused by this is discussed in Section 4.4, where there is an inconsistency in the pion and muon yield for incident proton beam kinetic energies above and below 10GeV.

3.2 Set Up

This study is based upon the proposed NF design. A liquid mercury jet is used as a target for an incident high energy proton beam as described in Section 2.2. For the simulation this is approximated by a cylindrical target of Mercury, length 200mm and radius 5mm [3].

In every simulation, the target and incident proton beam is centred on $x = 0$, $y = 0$, with the proton beam travelling in the $+z$ direction as displayed in Figure 3.1. For simplification purposes, the proton beam has been given negligible width and divergence; meaning all protons enter the target at the origin, $(x, y, z) = (0, 0, 0)$, travelling in only the z-direction, with velocity $(v_x, v_y, v_z) = (0, 0, v_z)$. However, in reality the beam is expected to have an RMS radius of 1.2mm and some finite divergence [3].

Unless otherwise specified, only the target dimensions, composition and proton beam kinetic energy have been adjusted between simulations.

Each proton is individual, whether or not it interacts with a given particle to create pion will not effect any of the other data. As each recorded event is independent, the systems collective behaviour can be statistically described by a Poisson distribution. Thus the error of a yield measurement can be taken as the standard deviation of the distribution, $\sqrt{n}$, where n is the total yield. All error bars for yields plotted on the included graphs are $\pm\sqrt{n}$. Due to the large data sets used, errors are often very small thus may be omitted.

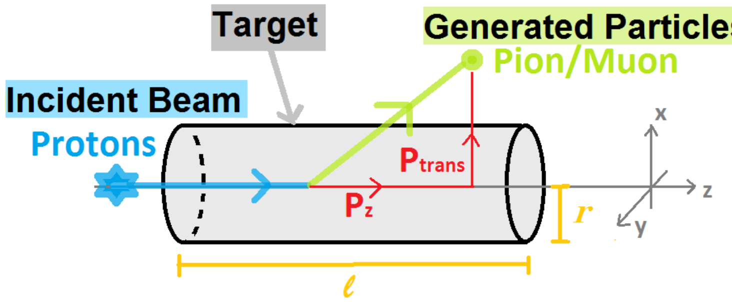

Figure 3.1: Orientation of the target and incident proton beam: both centred on $x = 0, y = 0$, with the beam travelling in the $+z$ direction. P_{trans} is the transverse component of the particles momentum as described by Equation 7.

3.3 Transverse Momentum

The transverse momentum component of each exiting particle is defined as

$$P_{transverse} = \sqrt{P_x^2 + P_y^2}, \tag{7}$$

as illustrated in Figure 3.1, where the three components of momentum (P_x, P_y, P_z) for each particle are measured by the detector. P_{trans} is important in determining whether a particle is successfully captured in the magnetic field surrounding the target, and thus obtaining the yield: small P_{trans} values are desired in order to reduce the necessary magnitude of the field.

The magnetic field will generate the Lorentz force on the moving charged particles of

$$\mathbf{F} = q(\mathbf{v} \times \mathbf{B}). \tag{8}$$

Where the particles velocity, $\mathbf{v}$, can be separated into transverse and longitudinal components: $\mathbf{v} = \mathbf{v}_{transverse} + \mathbf{v}_z$. The magnetic field, $\mathbf{B}$, is directed along the z-axis, hence it is parallel to $\mathbf{v}_z$ and the cross product of these terms will disappear. Thus only $\mathbf{v}_{transverse}$, the component of the particle's velocity directed radially outward, has been considered. The generated force, $\mathbf{F}$, will be perpendicular to both $\mathbf{v}_{transverse}$ and $\mathbf{B}$, which will cause the particles to orbit around the z-axis. Any component of velocity in the z-direction will not effect the orbit size, but act to move the particles along z, turning their orbit into a helical path. The particles can then be captured and accelerated down the beam pipe by further electric and magnetic fields as described in Section 2.2.

Equating Equation 8 to the force required for an object to travel in a circular orbit, $F = \gamma\frac{mv^2}{r}$, gives the maximum value of the allowed transverse momentum to be

$$P_{trans}^{\mathbf{Max}} = eBr_{max}, \tag{9}$$

Where relativistic momentum is $P = \gamma mv$, B is the magnitude of the magnetic field $\mathbf{B}$, and r_{max} is the radius of the shielding protecting the solenoid and, thus, the maximum allowable radius of each particle's trajectory in the x-y plane. If they circulate with a radius $r > r_{max}$, they may be absorbed by the shielding or avoid capture by the magnetic fields which are described in Section 2.2. The value of $P_{trans}^{\mathbf{Max}}$ for the system immediately surrounding the target in the NF design is found to be 450MeV/c where the beam pipe radius was 0.075m and magnetic field was of $B = 20$T .

The solenoids, used to create large magnetic fields, contain a high amount of stored energy which is dangerous. They are additionally large and difficult to construct. Thus the size of the magnetic field around the target is limited, consequently limiting $P_{trans}^{\mathbf{Max}}$.

There are limitations to this approximation because the magnetic field would be non-uniform and would partially penetrate into the target material, affecting the paths of all charged particles. Additionally some particles would have a negative z-component of momentum. In this case their helical path would be directed away from the beam line so they would not be captured. This is investigated in Section 5.2.

4 Initial Findings

4.1 Pions not Muons

Inside the target, pions are created from interactions between the protons in the incident beam and the nucleons in the target. As stated by Equations 5 and 6, with a probability of over 0.99877, all pions will decay into muons after an average time of 2.6×10^{-8}s [9]. For a pion travelling at the speed of light in a vacuum this would be at an average distance of 7.8m. As the method considered for pion production is at a high energy level, muons are created from the decays of high momentum pions in-flight, before they have lost a significant amount of their energy. The is seen in the simulation of the NF target, where the average momentum of 50,000 exiting pions is 650MeV/c from an incident proton beam of 15GeV: this corresponds to a speed of 0.98c.

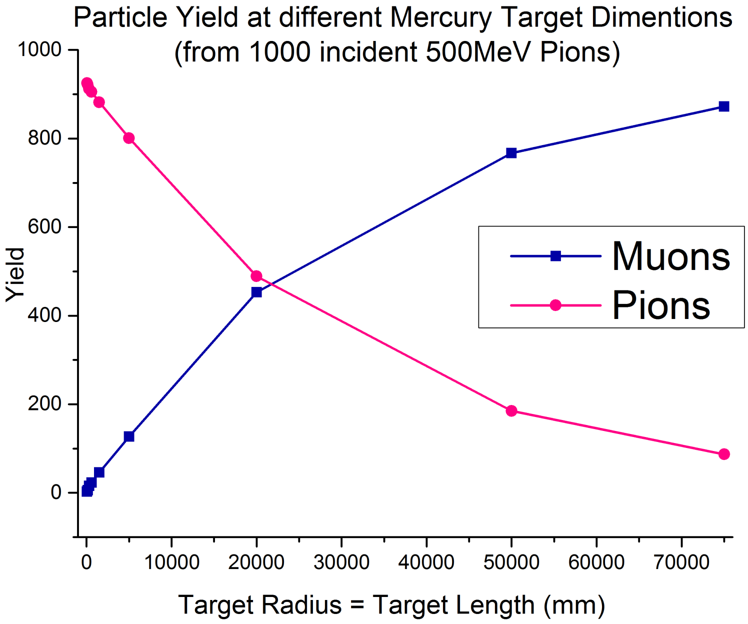

Figure 4.1: Graphs showing the total yields of pions and muons from a 500MeV beam of 1000 pions. Pions are incident on a cylindrical target of Mercury with varying dimensions, referring to both the length and radius of the target: from 60mm to 75m.

The pions considered in the simulation are relativistic but not travelling in a vacuum and will have a statistical distribution of speeds as they have different interactions. A large number of muons are thus created before 7.8m, but still at much larger distances than considered for the target dimensions: 0.2m. In order to find the distances taken for the high energy pions to decay into muons inside the target, a beam of pions with kinetic energy 500MeV was fired into a mercury target of varying thickness and the yield of pions and muons at the virtual detectors recorded. The results are shown in Figure 4.1 which displays that the yield of muons only significantly increases after around 20m, where the number of pions and muons becomes equal. This is larger by a factor of 100 than the length of mercury considered for the NF design. It is consequently not sensible to expect a large yield of muons at the virtual detectors encasing the simulated NF target.

In the NF design, the captured charged particles travel down the decay tube for 40.8m before being accelerated as described in Section 2.2. During this time, pions are able to decay into the required muons. It is therefore important to produce a high total yield with no preference to pions or muons, as the pions will certainly decay into muons. During this study, unless otherwise stated, the total yield refers to the total number both of pions and muons leaving the target and consequently counted at the detectors.

4.2 Target Geometry

The current target geometry in this simulation mimics the target design in the proposed NF unless otherwise stated. It is a 200mm long mercury cylinder of radius 5mm.

The effect of different target geometry on the total yield and mean transverse momentum component of pions and muons has been investigated. The target's radius and length have in turn been adjusted while simulating 1000 incident 15GeV protons on the target.

4.2.1 Target Radius

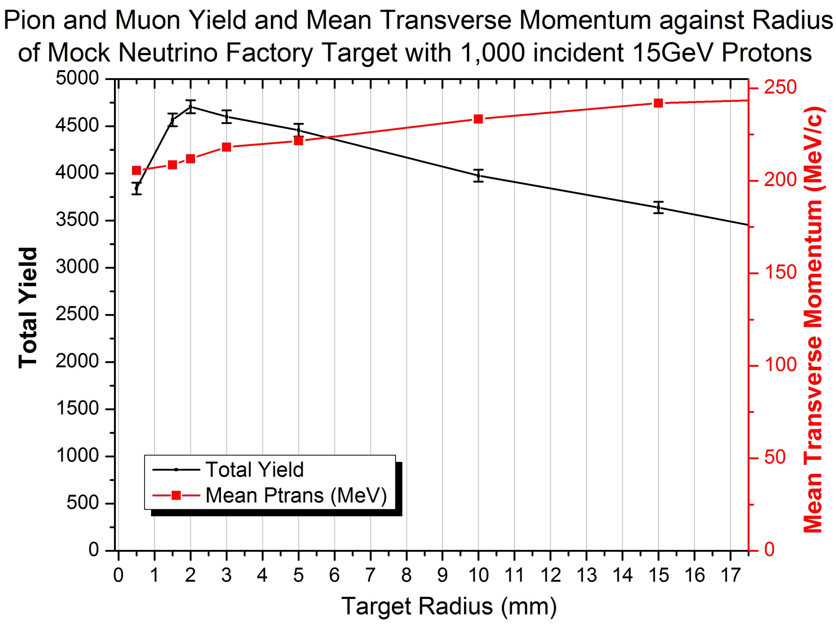

Figure 4.2: The yield of pions and muons and their mean transverse momentum against the radius of a cylindrical mercury target with length 200mm; from 1000 incident 15GeV protons.

Increasing the target radius while holding the length constant at 200mm displays a general decrease in total pion and muon yield as displayed in Figure 4.2. This is expected because an increased radius increases the amount of material the particles need to traverse in order to escape the target, as they all originate from the central axis $(x, y) = (0, 0)$. For a larger radius, the particles would deposit more energy in the material and an increased number would be stopped completely inside the target. In the simulation, the peak total yield can be seen at a target radius of 2mm, where a very small radius can be seen to reduce the total particle yield. This is because a larger proportion of protons would undergo elastic scattering out of a thinner target before inelastically scatting with a nucleon to produce the necessary pions. However, the optimum radius of 2mm would be unrealistic because the model has been simplified with a non-dispersive beam. In the NF design, the proton beam is expected to have a RMS radius of 1.2mm, and so the higher radius target in the NF design of 5mm is likely to be better than simulated 2mm [3].

Figure 4.2 additionally shows that pions leaving a target with a greater radius have a higher component of transverse momentum. This increase in mean momentum is caused because only those particles with a higher momentum are able to escape the thicker target. Additionally, prior to escape, particles undergo increased scattering by the target material, leading to a larger change in their overall direction. To increase the captured yield transverse momentum should be minimised. This is an additional reason the target should have a small radius.

4.2.2 Target Length

Increasing the target length while holding the radius at 5mm as displayed in Figure 4.3 increases the produced pion yield up to a maximum value: a yield of approximately 5600 pions and muons at a target length of 500mm. This maximum yield remains for any longer length of target as the majority of particles escape through the target edges quickly due to scattering. As the target has a small radius relative to length, only a small angle of divergence is needed for these particles to escape. The component of transverse momentum is shown to remain constant with length. As length changes only the z-direction, transverse components are independent of it.

The value of length proposed in the NF design of around 300mm seems sensible compared to the simulation data as is it approaching the point of maximum yield. However, a longer length should be considered as Figure 4.3 shows the considerable yield increase of 8% between target lengths of 300mm and 500mm.

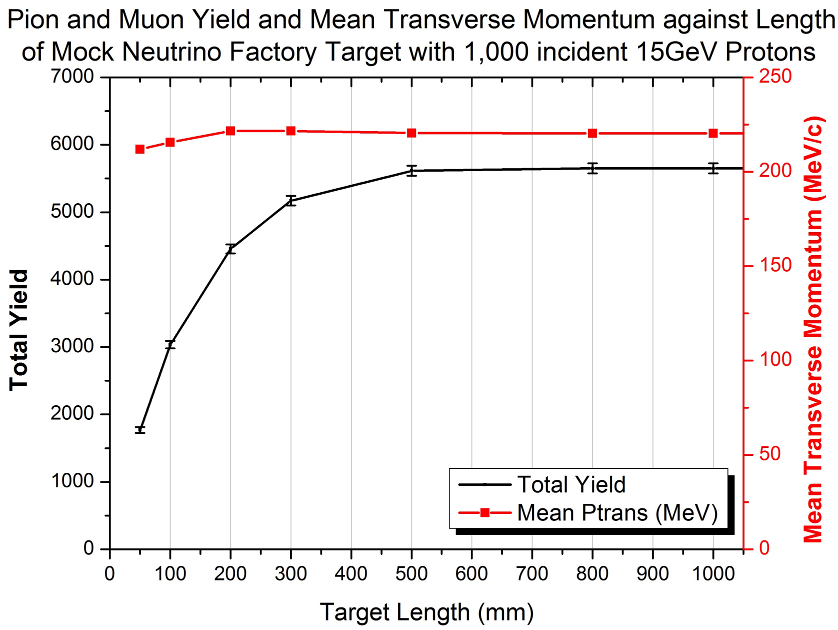

Figure 4.3: The yield of pions and muons and their mean transverse momentum against the length of a cylindrical mercury target with radius 5mm; from 1000 incident 15GeV protons.

4.3 Target Material Choice

The average distance an electron would travel in a material before losing $\frac{1}{e}$ of it's initial energy is defined as the elements radiation length and is used to normalize the distances traversed through different elements in high energy physics. The radiation lengths of each element, X_0, are plotted in Figure 4.4(A) against their atomic number. X_0 is a function of the material's density, atomic and mass numbers [15].

Noble gases have radiation lengths significantly higher than other elements. These are seen as the peaks of high radiation length in Figure 4.4(A). This is because noble gases have a very high ionisation potential and so have a low chemical re-activity. This means that incoming particles travel through these materials with very few interactions occurring, and thus losing their energy extremely slowly. Conversely, particles travelling through low X_0 materials will undergo a lot of interactions on average; making these materials suitable for target construction as they could produce a high intensity of pions and muons, as required by the NF . An increase of pion and muon yield corresponding to this was noted from the data collected in the simulation. This is displayed in Figure 4.4(B), where the pion and muon yield is plotted against the atomic number, Z, of the target material. The trend is analogous to the theoretical trends of X_0 in Figure 4.4(A), but inverted. This is because the shortest transition lengths lead to the most interactions per unit length and, thus, the highest yields of pions and muons.

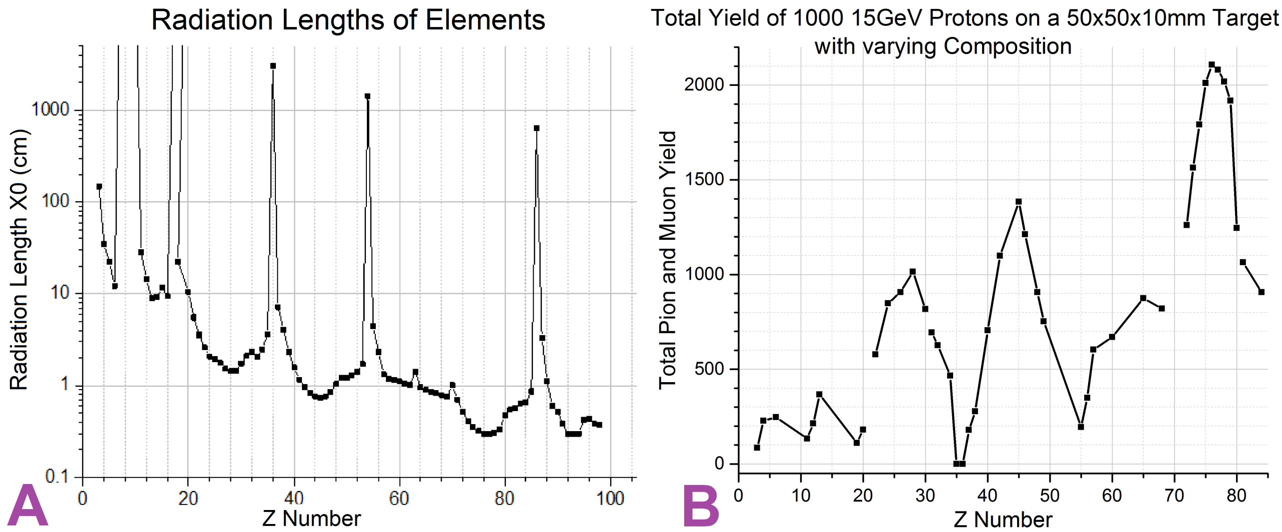

Figure 4.4: (A) The value of the radiation length, X_0 (cm), for each element in order of atomic number Z. This is the appropriate scaling length for high-energy electromagnetic cascades. (B) Total Yield of pions and muons from 1000 Protons with a kinetic energy of 15GeV incident on a $50 \times 50 \times 10$mm target made of varying element in order of atomic number Z.

Once the pions are created within the target, the known pion collision lengths are of importance. This is the length a pion would on average travel before loosing $\frac{1}{e}$ of its initial energy due to elastic and inelastic collisions [16]. These lengths generally have the same trends as X_0 but are specifically based on models and observations from pions. Elements with Z= 74-78 would stop Pions in the shortest distance as they have the shortest pion collision length. Therefore these elements would slow the Pions the fastest for a set length of material traversed. As it is of interest to slow the pions travelling in a transverse direction, the effect of adding these elements to the edges of the target will be investigated in Section 6.

4.4 Proton Beam Energy

As a general trend, an increase in the kinetic energy of the proton beam increases the total pion and muon yield. This effect was predicted in Section 2.1 due to the increased number of pairs of pions, $\pi^+\pi^-$, that can be produced in higher energy proton interactions. The data from the simulation showing the yield of pions and muons from a target simulating the NF design can be seen in Figure 4.5. Proton beam kinetic energies in the range $5 \rightarrow 15$GeV were investigated in depth, as these energies are stated as feasible in the current NF design indicated in Section 2.2 [3]. As the kinetic energy of the beam increases, the total pion yield increases, however less change is noted in muon yield as measurement is taken over a distance, 20cm, much smaller than would be the average distance travelled in a pions lifetime. Additionally, for higher initial kinetic energies, the velocity of pions is expected to be higher, leaving less time for muons to decay inside the target.

As described in Section 3, care should be taken just below 10GeV due to the different physics model used in the simulation. The change in yield that is expected can be seen in the data collected in Figure 4.5: increasing the proton beam kinetic energy form 9.5GeV to 10GeV gives an increase in yield of total pions and muons from 16944 ± 130 to 30827 ± 176, an increase of 82%. An identical beam energy increase of 0.5GeV below or above this region gives an approximate percentage increase in the total yield of 7% or 2% respectively. Therefore the jump in yield caused by the change of simulation model is very large and would be un-physical.

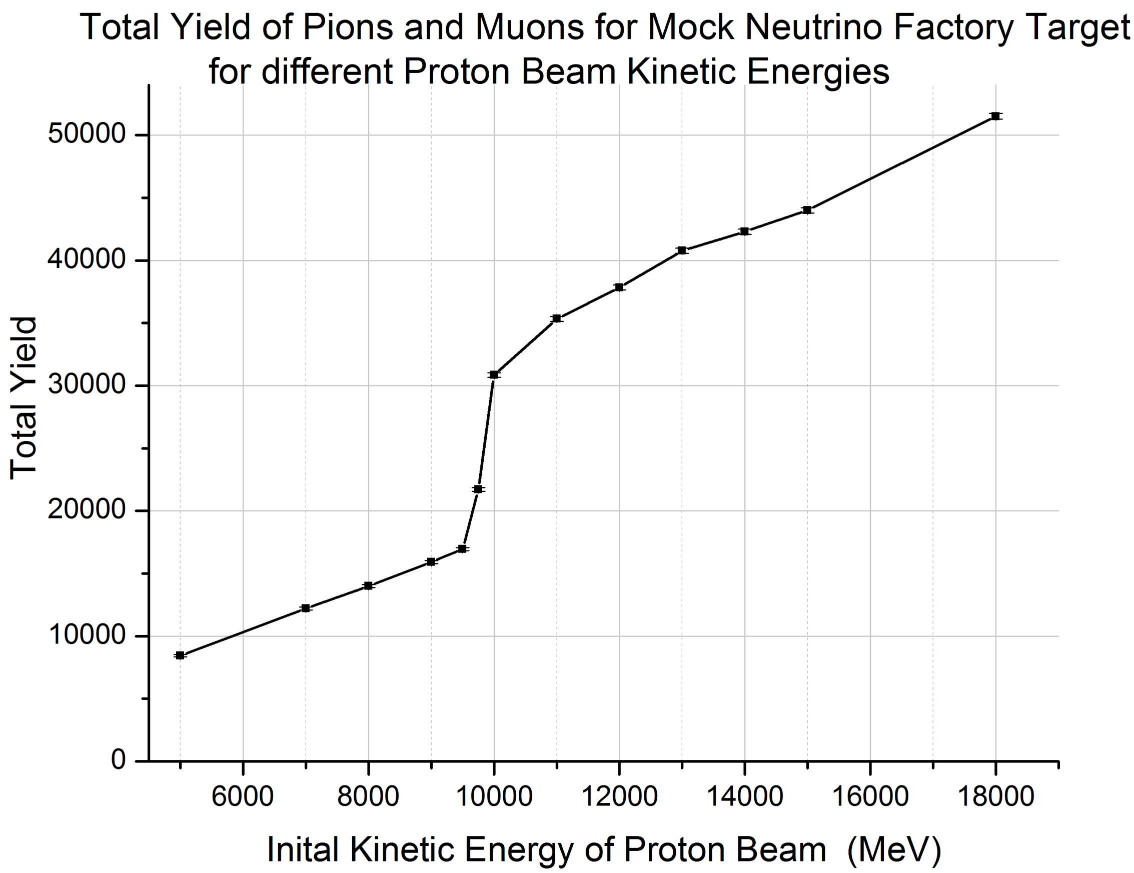

Figure 4.5: The yield of pions and muons against the kinetic energy of the proton beam; from a target simulating the NF design as described in Section 3.2 with 10,000 incident protons.

5 Optimisation

5.1 Transverse Momentum

The component of transverse momentum for each produced pion and muon is important in determining whether or not they can be captured and used in the beamline, as described in Section 3.3.

Assuming a positive value of P_z, all pions and muons with a transverse momentum component equal to or lower than $P_{trans}^{\mathbf{Max}}$, as stated in Equation 9, can theoretically be captured. The value of the transverse momentum component, P_{trans}, of each exiting particle is different but collectively they have a distribution due to the statistical nature of the interactions. This distribution changes with proton beam kinetic energy. Figure 5.1 displays histograms of the number of particles for each value of transverse momentum; plotted for three values of proton beam initial kinetic energy: 7, 11 and 18GeV. Aiming to reduce the transverse momentum, and subsequently increase the number of particles collected, it is important to have distribution with low RMS and mean P_{trans}: displayed in Figure 5.3. Both the mean and RMS P_{trans} are lower for an incident proton beam of kinetic energy $11GeV$ than for both 7GeV and 18GeV, illustrated quantitatively Figure 5.2. The mean P_{trans} value from a $18GeV$ is 15% higher, and a 7GeV beam 40% higher, than the 11GeV beam.

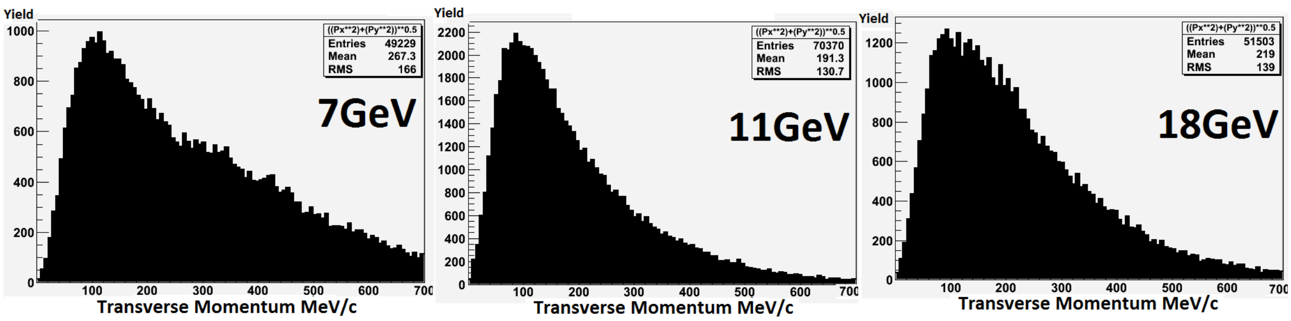

Figure 5.1: Comparison of histograms showing the distribution of the magnitude of transverse momentum for outgoing pions and muons from a mock NF target as described in Section 3.2. Data for three different initial proton beam kinetic energies: 7, 11 and 18GeV. The number of events (number of initial individual protons in the beam) for each energy is not equal in order to standardise the number data points: the statistical validity of the three distributions is approximately equal as each plot contains a total of around 50,000 data points, each representing an exiting pion or muon.

Beam Kinetic Energy GeV	Mean P_{trans} MeV/c	RMS P_{trans} MeV/c
7	267	166
11	191	130
18	219	139

Figure 5.2: Table displaying data from the three transverse momentum distributions in Figure 5.1. The mean and RMS P_{trans} from 7, 11 and 18GeV proton beams are given.

If the sole aim was to reduce P_{trans}, beam energies higher, and especially lower than approximately 11GeV should be avoided. However, the magnitude of the transverse momentum is only part of the problem in increasing the total captured yield. In Section 4.4 it was found high beam energies increase the total yield, therefore this must also be considered. Care should additionally taken as the energies considered are close to the 10GeV: the simulations point of discrepancy as described in Section 3.1.

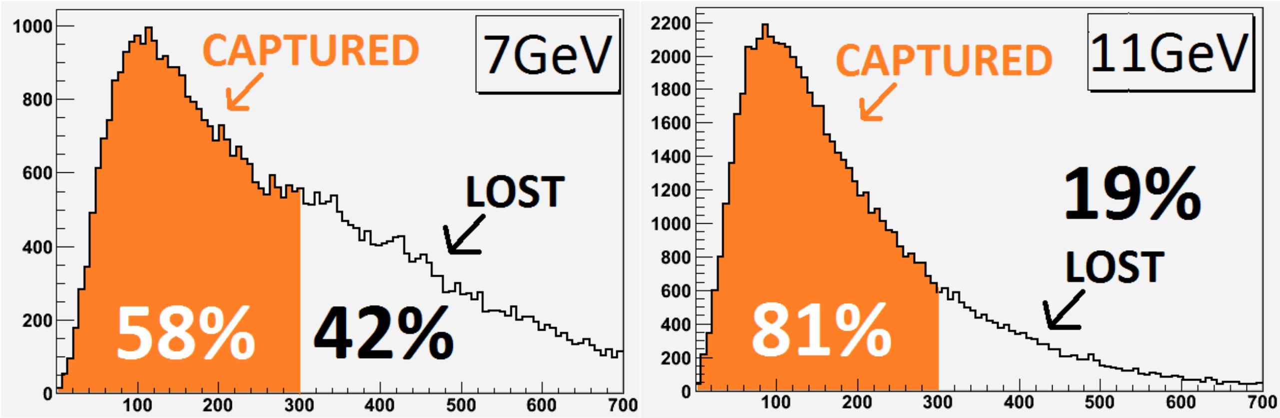

Figure 5.3: Example of the percentage of particles captured and lost for the different P_{trans} distributions in Figure 5.1. Displays that for $P_{trans}^{\mathbf{Max}} = 300\frac{MeV}{c}$, 81% of pions and muons are captured for a 11GeV initial proton beam kinetic energy, giving a tight P_{trans} distribution with a low mean, compared to only 58% for a 7GeV beam energy where the mean value of P_{trans} is lower and the distribution has a greater spread.

5.2 Total Captured Yield

Increasing the kinetic energy of the incident proton beam increases the total yield as discussed in Section 4.4. Additionally, Section 5.1 displays that there is an optimum value of beam kinetic energy to minimize the magnitude of particle transverse momentum allowing a higher proportion of particles to be captured and used. The total number of particles captured in the field is dependent on both these effects, therefore it is important to understand which is dominant in order to optimize the whole system.

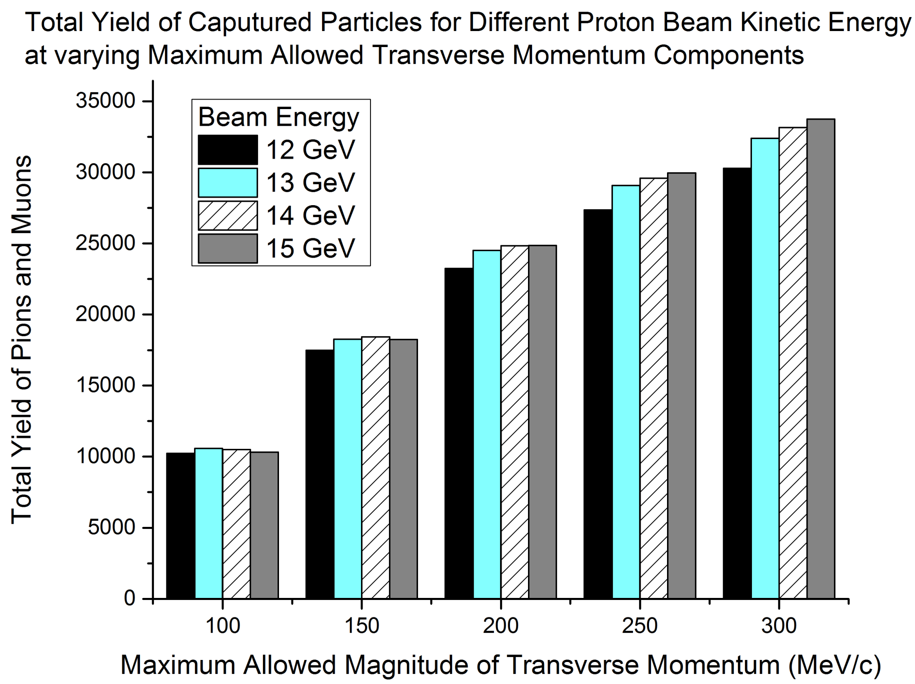

Figure 5.4: Comparison of the total captured yield of Pions and Muons for different initial proton beam energies: 12, 13, 14 and 15GeV. Data from 10,000 protons incident on NF mock target as described in Section 3.2.

Figure 5.4 displays the captured yield for 4 different values of beam kinetic energy dependent on the value of $P_{trans}^{\mathbf{Max}}$ for the target system design. For high values of $P_{trans}^{\mathbf{Max}}$ the captured yield increases with kinetic energy as shown in the column $P^{\mathbf{Max}}_{trans} = 300\frac{MeV}{c}$. In this case, and for larger values of $P^{\mathbf{Max}}_{trans}$, increasing the beam kinetic energy should be the priority, as the total captured yield increases with it. However, at lower values of $P^{\mathbf{Max}}_{trans}$, up to 200MeV/c, the captured yield is the same or decreased for higher kinetic energies. This shows that, dependent on the value of $P^{\mathbf{Max}}_{trans}$, there may be no advantage to using a higher kinetic energy.

The maximum component of transverse momentum for captured particles for the designed NF , $P^{\mathbf{Max}}_{trans}$, was calculated in Section 3.3 to be 450MeV/c. However, this could change during construction, dependent on the magnetic field strength of the target system and the beam pipe radius. It is displayed in Figure 5.5 that the total yield of pions and muons continues to increase for higher proton beam energies. However, the yield of captured particles, does not notably increase with an increased beam kinetic energy; this is true particularly for a target system with a low $P^{\mathbf{Max}}_{trans}$ as displayed by $P^{\mathbf{Max}}_{trans} = 150$MeV/c. For this $P^{\mathbf{Max}}_{trans}$ value, there would be no advantage in using a proton beam with kinetic energy higher than around $11GeV$ as the captured yield at beam energies above this point is approximately constant. For $P^{\mathbf{Max}}_{trans} = 250$MeV/c the captured yield does increase with beam energy, but this happens very slowly. Furthermore, higher energies cause the disadvantages of increased running costs, and an increase in the levels of activation the materials in the target system would receive-shortening their working lifetime. With these considerations, it may not be most effective to run the proton drive at maximal energy.

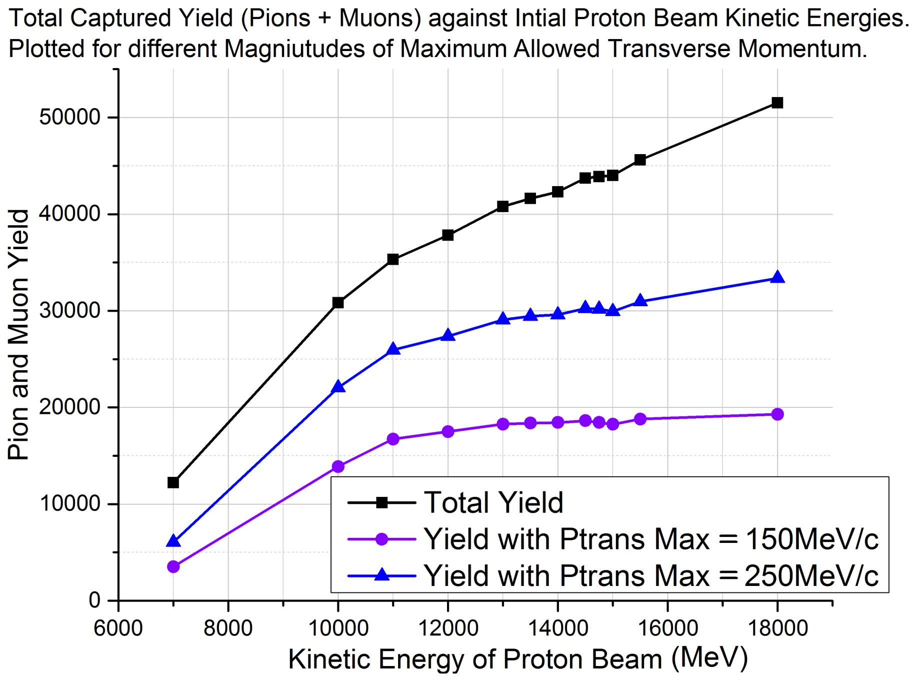

Figure 5.5: Total captured yield (Pions + Muons) against initial proton beam kinetic energies. Plotted for the total yield and the number of particles captured when $P^{\mathbf{Max}}_{trans}$ is 150MeV/c and 250MeV/c. Data from 10,000 protons incident on NF mock target as described in Section 3.2.

An additional requirement for capture would be for the particle's z-component of momentum to be in $+z$ direction. This would ensure that the helical path they are trapped into is directed down the beam pipe towards the accelerator. It was found that the percentage of the total pions and muons that have a negative P_z, and will thus be lost from the system, is 10% for higher energy 15GeV proton beams, and increases to 20% at beam energies of 5GeV. This increase in yield of particles that would enter the accelerator would be an advantage of using a higher energy beam.

6 Layering

Due to the previous observations noted in section 4.3 that materials with a low pion collision length reduce the momentum of particles the fastest. It was proposed that a target constructed of two concentric cylinders of different materials could improve the yield of captured particles.

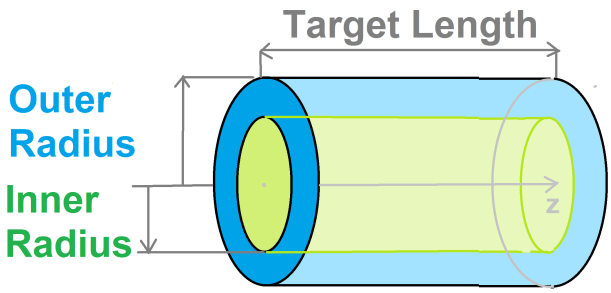

Figure 6.1: Diagram of the target constructed of 2 layers.

This theory was tested primarily with carbon and osmium. Although not practical materials to use, they have significantly different pion collision lengths of 39.12cm and 5.97cm respectively [16]. It is, thus, expected that any trends would be clearly seen. When arranged as in Figure 6.1, with an outer radius of 35mm and inner radius of 25mm, it is expected that an outer layer of osmium would reduce the particle's transverse momentum component. Figure 6.2(A) shows results for this arrangement, the mean direction of exiting pions from the ratio of P_{trans} and P_z, was predominately more forward. However, the key component in determining whether a particle is captured, P_{trans}, was not reduced with respect to the the carbon reference target, shown in Figure 6.2(B). Reductions in P_{trans} with respect to both the osmium inner and osmium reference targets can be seen, however, these targets produce a significantly higher yield. Therefore this is of no advantage unless the system has a very low $P_{trans}^{\mathbf{Max}}$ value. This is displayed in Figure 6.3, where the captured particle yield from the "carbon inner, osmium outer" target is comparable to the references, but never exceeds them.

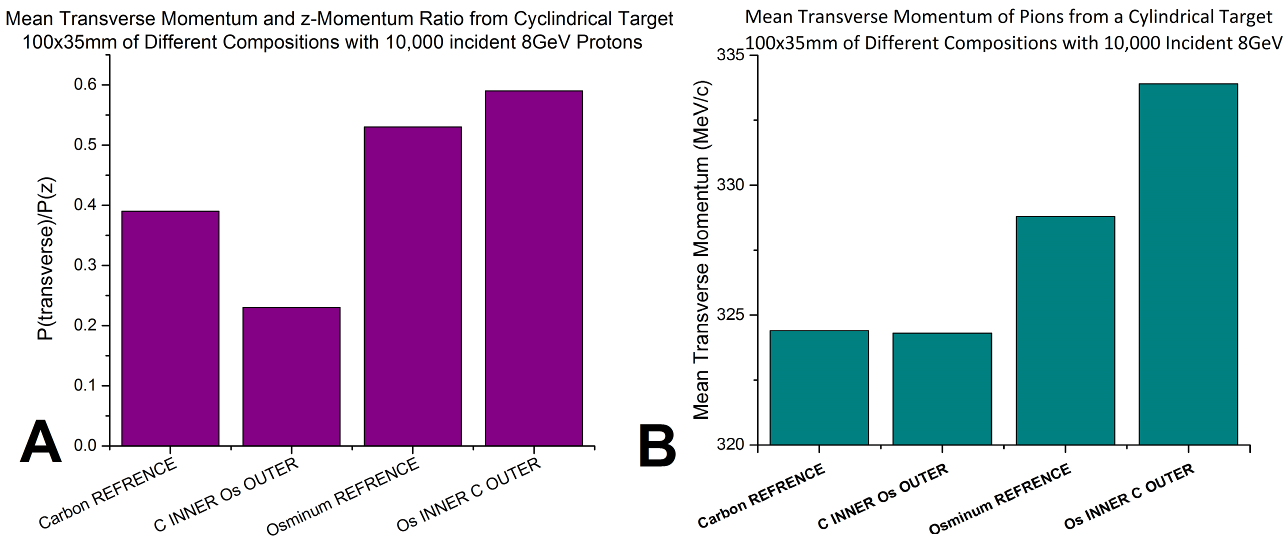

Figure 6.2: (A) Mean transverse pion momentum and z-Momentum ratio
(B) Mean transverse pion momentum
both from Cylindrical Target of Different Compositions, length 100mm, inner radius 25mm and outer radius 35mm, with 10,000 incident 8GeV Protons. Reference targets have radius 35mm.

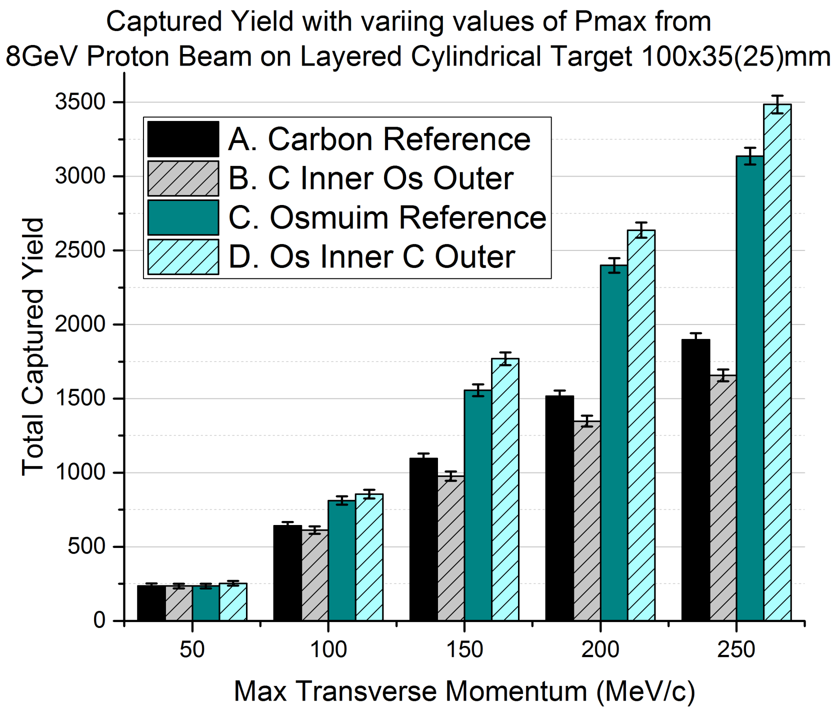

Figure 6.3: Comparison of the total captured yield of Pions and Muons from 10,000 8GeV protons for different layered targets with length 100mm, inner radius 25mm and outer radius 35mm.

Further investigations were carried out using tungsten and osmium as they have a closer value of radiation length, 6.94cm and 5.97cm respectively [16], so less of a discrepancy in total yield would be expected. As seen in Figure 6.4, almost no correlation between composition was found as all mean P_{trans} values were within 5% of each other. Additionally, the target with a thicker outer layer showed an unexpected increase in P_{trans} value; this may be due to statistical errors. Although a correlation has yet to be seen, it would be of interest to repeat the measurements with target radii similar those the proposed NF design.

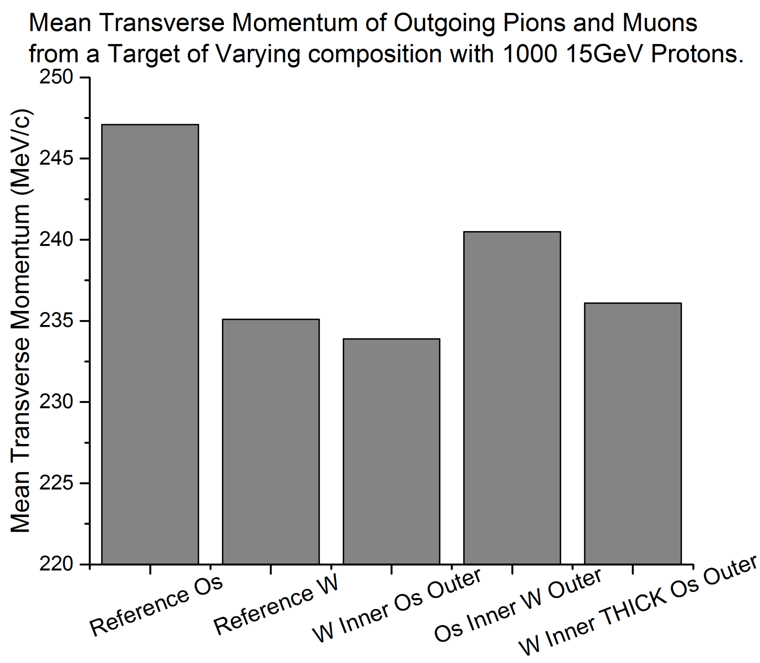

Figure 6.4: Mean transverse pion momentum from Cylindrical Target of Different Compositions of Tungsten (W) and Osmium (Os), length 200mm, inner radius 80mm and outer radius 120mm, with 1,000 incident 15GeV Protons. "THICK" target has outer radius 200mm.

7 Conclusion

The effect of target geometry, composition and proton beam energy were investigated by simulating pion production from a proton beam incident on a mercury target. This was carried out to increase the expected sensitivity at the proposed NF by increasing the yield of captured muons.

The geometry of the target was found to greatly influence the produced particle yield. For a 15GeV proton beam incident on a cylindrical mercury target, the optimum length for maximum particle yield was found to be 500mm which is larger than the currently proposed 300mm effective length. The optimum target radius was found to be 2mm although this is unrealistic as neglects the finite proton beam size. It is therefore proposed the 5mm radius suggested in the current NF design would be better than 2mm.

Due to the damage the target undergoes from the high energy beam, many material limitations are enforced. Materials were not fully investigated, however, the strong inverse relationship between particle yield and radiation length was noted.

Increasing the energy of the proton beam was found to generate the highest total muon yields, coupled with highest total momentums: particles are thus harder to capture and many will not be useful for neutrino production. Additionally, using a higher energy beam increases running costs and the levels of activation in the surrounding materials, causing safety and durability concerns. It was found that the optimum proton beam energy depends on the maximum allowed transverse momentum component of the system. If this was 150MeV/c there would be no advantage of a beam energy above 11GeV, or 13GeV for a maximum transverse momentum component of 250MeV/c. The calculated maximum transverse momentum component for the NF design was 450MeV/c, which is dependent on a very strong magnet being manufactured. The validity of these results would depend on the reliability of the simulation's models because the data is taken near the simulations 10GeV discrepancy.

A target composed of layers of different materials, osmium with tungsten or carbon, was investigated. It was proposed that a layer of lower radiation length material on the outer edges of the target would reduce the transverse component of exiting particle's momentum, however, no significant correlation was found. Further simulations should be completed to fully investigate this effect. Smaller target radii and other materials or compounds should be investigated. Additionally, as solid targets are not feasible due to the high power of the NF beam the manufacture of a layered target would have to be considered.

The results in this study are all generated by the same simulation and same physics models. They should be repeated with alternate models to gain a more comprehensive insight into the interactions occurring. As described in Section 3.1, a model has yet to be found which accurately describes interactions taking place at high energies. This suggests large limitations in the reliability of the results, demonstrated by the discrepancy seen at energies of 10GeV. Therefore the errors quoted $\pm\sqrt{n}$ should be taken as interpretations of the statistical error only and the experimental compatibility of the results considered with caution.

Following these investigations, the proposed effective length of the NF should be revised in order to fully maximize the particle yield. The optimum beam energy should be further investigated using alternate physics models in order to test the reliability of the proposed data. Additionally, quantitative estimations of the negative impact high beam energies have on the system's lifetime and running costs should be made. Further studies should be taken to investigate targets composed of layered materials in order to see whether the proposed reduction to transverse momentum and thus increase in captured particle yield could be generated by using low X_0 materials on the cylinder edge.

Word Count: 5977

References

[1] Felice Laake, 20/12/2013, 'ISIS: Making Muons for a quarter of a century', URL: http://nmi3.eu/muon-research/, ISIS, Integrated Infrastructure Initiative for Neutron Scattering and Muon Spectroscopy

[2] Robert H. Heffner, 1984, 'Muon Sources for Solid-state Research By National Research Council (U. S.). Subcommittee on Muon Sources for Solid State Research', National Academies.

[3] The IDS-NF collaboration, 24th December 2013, 'International Design Study for the Neutrino Factory- Reference Design Report', IDS-NF , Draft 1.

[4] Spallation Neutron Source, Oak Ridge National Laboratory, URL: https://neutrons. ornl.gov/sns

[5] Science and Technology Facilities council, 2015, 'Muons', URL: http://www.isis.stfc.ac.uk /groups/muons/muons3385.html

[6] The Paul Scherrer Institute, URL: https://www.psi.ch/

[7] W. R. Leo, 1993, 'Techniques for Nuclear and Particle Physics Experiments: A How-to Approach', 2nd Revised Edition, Springer-Verlag, page 130.

[8] Tavernier, Stefaan, 2010, 'Experimental Techniques in Nuclear and Particle Physics', Springer, Chapter 2, page 271.

[9] K.A. Olive et al. (Particle Data Group), 2014, 'Light Unflavored Mesons', Chin. Phys. C38, 090001 (URL: http://pdg.lbl.gov), page 1.

[10] J. Beringer et al. Particle Data Group, 2012, 'Muon', URL:http://pdg.lbl.gov/ 2012/listings/rpp2012-list-muon.pdf, PR D86, 010001, page 2.

[11] I. Efthymiopoulos et al, Oct 2008, 'MERIT - The high intensity liquid mercury target experiment at the CERN PS', MERIT Collaboration, DOI: 10.1109/NSSMIC.2008.4775051, Conference: C08-10-18, p.3302-3305

[12] C. Fazioa, June 2008, 'The MEGAPIE-TEST project: Supporting research and lessons learned in first-of-a-kind spallation target technology', Nuclear Engineering and Design Volume 238, Issue 6 Pages 1471–1495. DOI:10.1016/j.nucengdes.2007.11.006

[13] Tom Roberts, December 2013, 'G4beamline User's Guide 2.16', URL: http://muonsinc.com /muons3/g4beamline/ G4beamlineUsersGuide.pdf, Muons, Inc.

[14] Geant4, Last Updated 27 Mar 2013, 'Reference Physics Lists', URL: https://geant4.web.cern.ch /geant4/support/

[15] J. Beringer et al. Particle Data Group, 2012, '31. Passage of Particles Through Matter', PR D86, 010001, page 18.

[16] Particle Data Group, Last revised 12 August 2014, 'Atomic and Nuclear Properties of Materials for more than 300 materials ', URL: http://pdg.lbl.gov/2015/AtomicNuclearProperties/